



## Letter

# Multiwavelength excited novel red-emitting phosphor $\text{Eu}^{3+}$ -activated $\text{Li}_2\text{Zn}_2(\text{MoO}_4)_3$

Xianghong He\*, Mingyun Guan, Chunyong Zhang, Tongming Shang, Ning Lian, Yan Yao

School of Chemistry and Environmental Engineering, Jiangsu Teachers University of Technology, Changzhou, Jiangsu 213001, China

## ARTICLE INFO

## Article history:

Received 18 April 2011

Received in revised form 17 June 2011

Accepted 17 June 2011

Available online 24 June 2011

## Keywords:

Phosphors

Solid state reactions

X-ray diffraction

Luminescence

## ABSTRACT

$\text{Eu}^{3+}$ -activated  $\text{Li}_2\text{Zn}_2(\text{MoO}_4)_3$  multiwavelength excited red-emitting phosphors were synthesized via a solid state reaction. The structure and photoluminescence characteristics were investigated by X-ray powder diffraction and fluorescent spectrophotometry, respectively. The excitation spectrum included a strong broadband ranging from 250 to 350 nm and some sharp peaks at 363, 384, 395, 465, and 533 nm, which matches the radiations of near-UV or blue light-emitting diodes chip well. Upon excitation either of near-UV or blue even green light, the intense red emission with 615 nm peak can be observed, which is ascribed to the  ${}^3\text{D}_0$ – ${}^7\text{F}_2$  transition of  $\text{Eu}^{3+}$  ions. The chromaticity coordinates ( $x=0.65$ ,  $y=0.34$ ) of the as-obtained phosphor is very close to the National Television Standard Committee standard values ( $x=0.67$ ,  $y=0.33$ ). All these characteristics suggest that  $\text{Eu}^{3+}$ -doped  $\text{Li}_2\text{Zn}_2(\text{MoO}_4)_3$  wavelength-conversion material to be suitable candidate red component for phosphor-converted white light-emitting diodes.

© 2011 Elsevier B.V. All rights reserved.

## 1. Introduction

In recent years, phosphor-converted white light-emitting diodes (pc-white-LEDs) are the subject of increasing interest due to their long lifetime, high energy-efficiency, reliability, durability and environmentally friendly characteristics [1–4]. The pc-white-LEDs are usually fabricated by a near-UV or blue emitting semiconductor chip coated with wavelength-conversion luminescent materials layer. The eventual performance of pc-white-LEDs devices strongly depends on the luminescence properties of the phosphors used. Therefore, the state-of-the-art pc-white-LEDs devices would be notably advanced by the discovery of phosphor materials that are optimized for pc-white-LEDs. The most frequently used red-emitting phosphor for near-UV LEDs is  $\text{Y}_2\text{O}_2\text{S}:\text{Eu}^{3+}$ . However,  $\text{Y}_2\text{O}_2\text{S}:\text{Eu}^{3+}$  phosphor has poor absorption in near-UV region where LED chips emission occurs. A good strategy to overcome this problem is to search for a host lattice that can absorb energy efficiently in the near-UV region and transfer the energy to the activator, resulting in emission in the red region (host sensitized emission) [5,6]. Hence, there has been a widespread and growing interest in the discovery or development of novel families of red-emitting phosphors with strong absorption in the near-UV to blue spectral region [5–11].

Double molybdates own excellent thermal and hydrolytic stability and are suitable as host for optical materials [12–14].  $\text{Eu}^{3+}$

is an excellent red-emitting activator in many classic phosphors such as  $\text{Y}_2\text{O}_2\text{S}:\text{Eu}^{3+}$ ,  $\text{YVO}_4:\text{Eu}^{3+}$ . Therefore,  $\text{Eu}^{3+}$ -doped double molybdates phosphors have attracted a great deal of attention because they exhibit intense charge-transfer absorption bands in near-UV and effective 4f–4f transitions of  $\text{Eu}^{3+}$  [10–14]. Following the excitation in the near-UV, the energy absorbed by the host can be transferred to  $\text{Eu}^{3+}$  ions via a non-radiative mechanism, which leads to pure red emission. As a member of this family,  $\text{Li}_2\text{Zn}_2(\text{MoO}_4)_3$  was recently found to be a kind of tunable refractive index materials in the middle- and near-ultraviolet region [15]. Solodovnikov et al. explored the scintillating characteristics of  $\text{Li}_2\text{Zn}_2(\text{MoO}_4)_3$  crystal [16,17]. This compound is expected to be used as a host lattice, because  $\text{Li}^+$  and  $\text{Zn}^{2+}$  are randomly distributed over the same cationic sublattice, resulting in a local lattice disorder around the activator ions [15,16,18,19]. However, less information is available concerning the luminescence of  $\text{Li}_2\text{Zn}_2(\text{MoO}_4)_3$  based materials. Herein, we synthesized  $\text{Eu}^{3+}$ -activated  $\text{Li}_2\text{Zn}_2(\text{MoO}_4)_3$  red-emitting phosphors and investigated their composition-dependent photoluminescence properties.

## 2. Experimental procedures

$\text{Eu}^{3+}$ -doped  $\text{Li}_2\text{Zn}_2(\text{MoO}_4)_3$  phosphors with nominal composition of  $\text{Li}_{2-2t}\text{Zn}_{1.90+t}(\text{MoO}_4)_3:0.05\text{Eu}^{3+}, 0.05\text{Li}^+$  (abbreviated as LZMO: $\text{Eu}^{3+}$  hereafter,  $-0.10 \leq t \leq 0.30$ ) were prepared through a typical solid state reaction in air. The starting materials,  $\text{Li}_2\text{CO}_3$  (98.0%),  $\text{ZnO}$  (99.95%),  $\text{MoO}_3$  (99.5%) and  $\text{Eu}_2\text{O}_3$  (99.99%) were thoroughly mixed in the stoichiometric ratio by grinding for 0.5 h in an agate mortar and pressed into pellets with diameter of 12 mm and thickness of 2–3 mm. A small amount of acetone was added during the grindings in order to obtain homogenous mixtures. The pellets were sintered at 600 °C in air for 2 h in a muffle

\* Corresponding author. Tel.: +86 519 8695 3273; fax: +86 519 8695 3269.

E-mail address: [hexh@jstu.edu.cn](mailto:hexh@jstu.edu.cn) (X. He).

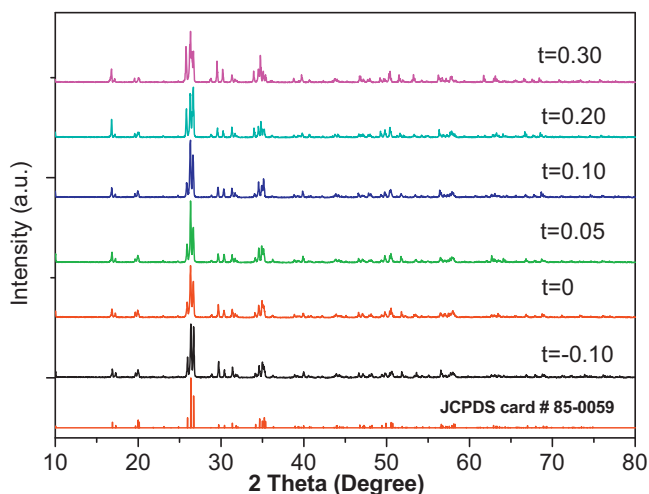


Fig. 1. XRD patterns of  $\text{Li}_{2-2t}\text{Zn}_{1.90+t}(\text{MoO}_4)_3:0.05\text{Eu}^{3+},0.05\text{Li}^+$  ( $-0.10 \leq t \leq 0.30$ ) phosphors and JCPDS card no. 85-0059 as a reference.

furnace, followed by calcination at  $800^\circ\text{C}$  for another 4 h. Finally, the samples are ground into powder for characterizations.

The powder samples were characterized by X-ray powder diffraction (XRD), and fluorescent spectrophotometry. The XRD was carried out with a Japan Rigaku D/max-rA rotation anode X-ray diffractometer, using Ni-filtered  $\text{Cu K}\alpha$  radiation. A scan rate of  $0.02^\circ/\text{s}$  was applied to record the patterns in the  $2\theta$  range  $10\text{--}90^\circ$ . Excitation and emission spectra of powders were recorded using fluorescence spectrofluorometer (Varian Cary-Eclipse). All the measurements were performed at room temperature.

### 3. Results and discussion

The body colors of as-obtained phosphor powders are white. XRD patterns of  $\text{LZMO}:\text{Eu}^{3+}$  with various  $t$  values are shown in Fig. 1. All the peaks can be indexed to isostructural  $\text{Li}_2\text{Co}_2(\text{MoO}_4)_3$  phase (JCPDS no. 85-0059) with orthorhombic system and space group  $Pnma$  [18]. The incorporation of  $\text{Eu}^{3+}$  ions with low content (5.0 mol%) does not clearly alter the lattice structure of host. As the  $t$  value varies, XRD patterns were found to be similar without showing discernable shifting. No impurity phases related to the starting materials and intermediates were found, indicating that the as-synthesized compounds are of single phase. In LZMO host lattice, Li atoms could be partially substituted by Zn atoms, resulting in the forming of solid solution in LZMO ( $-0.10 \leq t \leq 0.30$ ) compound [18,19]. Thus, the framework structure of  $\text{LZMO}:\text{Eu}^{3+}$  retains stable with  $t$  ranging from  $-0.10$  to  $0.3$ , which is in good agreement with previous reports [15,16].

Fig. 2 displays the excitation spectra of  $\text{LZMO}:\text{Eu}^{3+}$  phosphors with various  $t$  values. When the  $t$  value changed from  $-0.10$  to  $0.30$ , the excitation spectra were similar except that the intensity of excitation peaks. Under monitoring at  $615\text{ nm}$  corresponding to  $^5\text{D}_0 \rightarrow ^5\text{F}_2$  emission of  $\text{Eu}^{3+}$  ions, the phosphors exhibit one broad and strong band as well as some sharp peaks. The broad band between  $230$  and  $350\text{ nm}$  can be attributed to the combinations of charge-transfer (CT) transitions from  $\text{Mo}^{6+}-\text{O}^{2-}$  and  $\text{Eu}^{3+}-\text{O}^{2-}$  [20]. The sharp peaks beyond  $350\text{ nm}$  are ascribed to the typical  $\text{Eu}^{3+}$  intra- $4f^6$  transitions, including the peaks with maximum at  $363\text{ nm}$  ( $^7\text{F}_0 \rightarrow ^5\text{D}_4$ ),  $384\text{ nm}$  ( $^7\text{F}_0 \rightarrow ^5\text{G}_{2-4}$ ),  $395\text{ nm}$  ( $^7\text{F}_0 \rightarrow ^5\text{L}_6$ ),  $418\text{ nm}$  ( $^7\text{F}_0 \rightarrow ^5\text{D}_3$ ),  $465\text{ nm}$  ( $^7\text{F}_0 \rightarrow ^5\text{D}_2$ ), and  $535\text{ nm}$  ( $^7\text{F}_1 \rightarrow ^5\text{D}_1$ ), respectively. The narrowband  $4f-4f$  transitions of  $\text{Eu}^{3+}$  are more intense than the CT broad band. Of these excitation lines, the intensities of the  $395$ ,  $383$  and  $465\text{ nm}$  excitation peaks are much stronger than the others, which indicates that near-UV and blue LEDs are efficient pumping sources in obtaining  $\text{Eu}^{3+}$  emissions.

Emission spectra of  $\text{LZMO}:\text{Eu}^{3+}$  phosphors with different  $t$  values are depicted in Fig. 3. Upon excitation of  $395\text{ nm}$  near-UV or

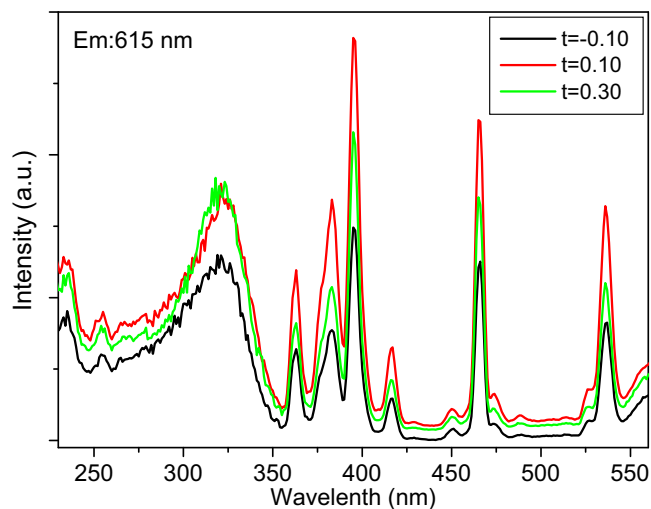


Fig. 2. Excitation spectra of  $\text{Li}_{2-2t}\text{Zn}_{1.90+t}(\text{MoO}_4)_3:0.05\text{Eu}^{3+},0.05\text{Li}^+$  phosphors with various  $t$  values (monitoring wavelength  $\lambda_{\text{em}} = 615\text{ nm}$ ).

$465\text{ nm}$  blue light, the samples show identical spectral emission except for the difference in intensity, which is composed of several narrow spectral lines in the range  $500\text{--}750\text{ nm}$ . The emission peaks are observed at  $592$ ,  $615$ ,  $654$ ,  $702\text{ nm}$ , corresponding to the  $^5\text{D}_0 \rightarrow ^7\text{F}_1$ ,  $^5\text{D}_0 \rightarrow ^7\text{F}_2$ ,  $^5\text{D}_0 \rightarrow ^7\text{F}_3$ ,  $^5\text{D}_0 \rightarrow ^7\text{F}_4$  transitions of  $\text{Eu}^{3+}$ , respectively. Of these peaks, the red emission peak at  $615\text{ nm}$  is stronger than the other peaks, which is advantageous to obtain good chromaticity coordinates near the National Television Standard Committee (NTSC) standard values [21]. The ratio of the integrated intensities of  $^5\text{D}_0 \rightarrow ^7\text{F}_2$  to  $^5\text{D}_0 \rightarrow ^7\text{F}_1$  (i.e. the asymmetric ratio) can be used as an index to measure the site symmetry of  $\text{Eu}^{3+}$  ions [22]. Generally, the larger the asymmetric ratio, the lower the local symmetry [23]. The asymmetric ratios of  $\text{LZMO}:\text{Eu}^{3+}$  phosphors with  $t$  value  $-0.10$ ,  $0.10$  and  $0.30$  were calculated to be  $7.16$ ,  $5.65$ , and  $5.64$ , respectively. The larger asymmetric ratios imply that  $\text{Eu}^{3+}$  ions occupy a non centro-symmetric site in LZMO host.  $\text{Zn}^{2+}$  is coordinated with six oxygen atoms to form a distorted octahedron with different Zn–O bond lengths in LZMO lattice [18]. The radius of  $\text{Eu}^{3+}$  ion ( $95\text{ pm}$ , sixfold coordination) is relatively closer to that of  $\text{Zn}^{2+}$  ion ( $74\text{ pm}$ , sixfold coordination). Thus,  $\text{Eu}^{3+}$  ions were supposed to occupy the  $\text{Zn}^{2+}$  crystallographic sites rather than

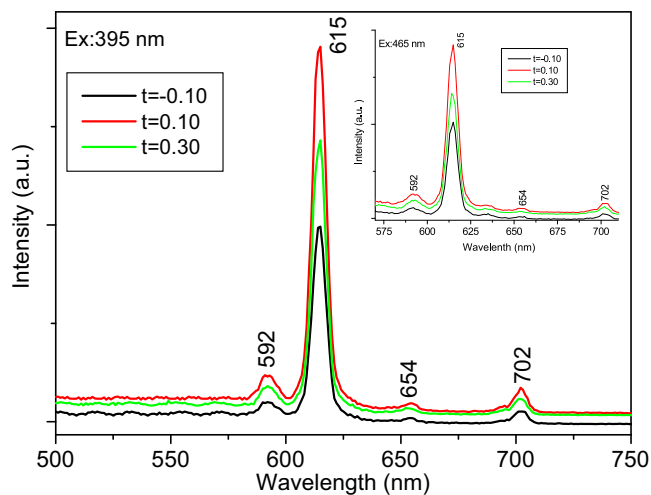


Fig. 3. Emission spectra of  $\text{Li}_{2-2t}\text{Zn}_{1.90+t}(\text{MoO}_4)_3:0.05\text{Eu}^{3+},0.05\text{Li}^+$  phosphors with different  $t$  values under various excitation wavelength  $\lambda_{\text{ex}} = 395\text{ nm}$  and  $\lambda_{\text{ex}} = 465\text{ nm}$  (the inset).

Li<sup>+</sup> or Mo<sup>6+</sup> sites of LZMO:Eu<sup>3+</sup>. Therefore, the emission spectra of LZMO:Eu<sup>3+</sup> were dominated by pure red peak at 615 nm.

As shown in Fig. 3, with increasing of *t* value, the red-emitting intensity of LZMO:Eu<sup>3+</sup> phosphors first increases, reaching a maximum value when *t* is 0.10, and then decreases accompanying a further increasing of *t* value. This can be explained as follows. As *t* value increases, the molar ratio of Li/Zn decreases, which will result in the forming of vacancies in cation sites to balance the excess positive charge [15]. The presence of vacancies can promote the energy transfer from excited carriers in LZMO host lattice to Eu<sup>3+</sup> activator, and then enhance the luminescence.

The commission International de l'Eclairage (CIE) chromaticity coordinates of LZMO:Eu<sup>3+</sup> are calculated to be *x* = 0.65, *y* = 0.34, which is closer to the standard of the NTSC (*x* = 0.67, *y* = 0.33) than that of commercial red-emitting phosphor of Y<sub>2</sub>O<sub>2</sub>S:Eu<sup>3+</sup> (0.63, 0.35).

#### 4. Conclusions

Multiwavelength excited narrow line red-emitting phosphors Li<sub>2-2*t*</sub>Zn<sub>1.90+*t*</sub>(MoO<sub>4</sub>)<sub>3</sub>:0.05Eu<sup>3+</sup>, 0.05Li<sup>+</sup> were successfully prepared via the conventional solid-state reaction. This double molybdate based phosphor presents the broad absorption from 230 to 350 nm, along with multiple excitation peaks at 363, 384, 395, 465, and 533 nm. Upon excitation with UV, near-UV rays or blue even green light, the phosphors exhibit strong red luminescence with CIE chromaticity coordinates (*x* = 0.65, *y* = 0.34). All these suggest Eu<sup>3+</sup>-activated Li<sub>2</sub>Zn<sub>2</sub>(MoO<sub>4</sub>)<sub>3</sub> to be promising phosphor for pc-white-LEDs application.

#### Acknowledgments

The authors thank Dr. Jinping Huang of Shanghai Normal University for assistance with the XRD measurements. This work

was financially supported by the Natural Science Research Project of the Jiangsu Higher Education Institutions (08KJD150014), the QingLan Project of the Jiangsu Province (2008), and the Students' Sci-tech Innovation Foundation of Jiangsu Teachers University of Technology (KYX10008).

#### References

- [1] S. Nakamura, T. Mukai, M. Senoh, *Appl. Phys. Lett.* 64 (1994) 1687.
- [2] S. Ye, F. Xiao, Y.X. Pan, Y.Y. Ma, Q.Y. Zhang, *Mater. Sci. Eng. R* 71 (2010) 1.
- [3] H.A. Höpfe, *Angew. Chem. Int. Ed.* 48 (2009) 3572.
- [4] L. Chen, C.C. Lin, C.W. Yeh, R.S. Liu, *Materials* 3 (2010) 2172.
- [5] R. Zhu, Y. Huang, H.J. Seo, *J. Am. Ceram. Soc.* (2011), DOI: 10.1111/j.1551-2916.2011.04502.x.
- [6] S. Yan, Y. Chang, W. Hwang, Y. Chang, M. Yoshimura, C. Hwang, *J. Alloys Compd.* 509 (2011) 5777.
- [7] X.H. He, M.Y. Guan, N. Lian, J.H. Sun, T.M. Shang, *J. Alloys Compd.* 492 (2010) 452.
- [8] M. Nyman, M.A. Rodriguez, L.E. Shea-Rohwer, J.E. Martin, P.P. Provencio, *J. Am. Chem. Soc.* 131 (2009) 11652.
- [9] Y. Yang, X. Li, W. Feng, W. Yang, W. Li, C. Tao, *J. Alloys Compd.* 509 (2011) 845.
- [10] X.H. He, M.Y. Guan, J.H. Sun, N. Lian, T.M. Shang, *J. Mater. Sci.* 45 (2010) 118.
- [11] P. Dai, X. Zhang, X. Li, G. Wang, C. Zhao, Y. Liu, *J. Lumin.* 131 (2011) 653.
- [12] G. Benoit, J. Véronique, A. Arnaud, G. Alain, *Solid State Sci.* 13 (2011) 460.
- [13] Z. Xu, C. Li, G. Li, R. Chai, C. Peng, D. Yang, J. Lin, *J. Phys. Chem. C* 114 (2010) 2573.
- [14] J. Liao, H. You, B. Qiu, H. Wen, R. Hong, W. You, Z. Xie, *Curr. Appl. Phys.* 11 (2011) 503.
- [15] L.P. Xue, Y.J. Wang, P.W. Lv, D.G. Chen, Z. Lin, J.K. Liang, F. Huang, Z. Xie, *Cryst. Growth Des.* 9 (2009) 914.
- [16] S.F. Solodovnikov, Z.A. Solodovnikova, E.S. Zolotova, L.I. Yudanova, T.Y. Kardash, A.A. Pavlyuk, V.A. Nadolinny, *J. Solid State Chem.* 182 (2009) 1935.
- [17] V.A. Nadolinny, N.V. Chernei, A.V. Sinitsyn, A.A. Pavlyuk, S.F. Solodovnikov, *J. Struct. Chem.* 49 (2008) 859.
- [18] L.P. Xue, D.G. Chen, Z. Lin, P.W. Lv, F. Huang, J.K. Liang, *J. Alloys Compd.* 430 (2007) 67.
- [19] L.P. Xue, Z. Lin, F. Huang, J.K. Liang, *Chinese J. Struct. Chem.* 26 (2007) 1208.
- [20] M.M. Haque, D. Kim, *Mater. Lett.* 63 (2009) 793.
- [21] Z. Wang, H. Liang, J. Wang, M. Gong, Q. Su, *Appl. Phys. Lett.* 89 (2006) 071921.
- [22] S. Fujihara, K. Tokumo, *Chem. Mater.* 17 (2005) 5587.
- [23] L.X. Yu, H.W. Song, S.Z. Lu, Z.X. Liu, L.M. Yang, X.G. Kong, *J. Phys. Chem. B* 108 (2004) 16697.